



## Technical note: A comparison of methods for estimating coccolith mass

Celina Rebeca Valença<sup>1</sup>, Luc Beaufort<sup>2</sup>, Gustaaf Marinus Hallegraef<sup>3</sup>, and Marius Nils Müller<sup>1,4</sup>

<sup>1</sup>Department of Oceanography, Federal University of Pernambuco, Recife, 50740-550, Brazil

<sup>2</sup>Aix-Marseille University, CNRS, IRD, INRAE, CEREGE, Aix-en-Provence, France

<sup>3</sup>Institute for Marine and Antarctic Studies, University of Tasmania, Private Bag 129, TAS 7001, Australia

<sup>4</sup>Macau Environmental Research Institute, Macau University of Science and Technology, Macau SAR, China

**Correspondence:** Marius Nils Müller (mariusnmuller@gmail.com)

Received: 20 December 2023 – Discussion started: 22 December 2023

Revised: 25 February 2024 – Accepted: 29 February 2024 – Published: 28 March 2024

**Abstract.** The fossil record of coccolithophores dates back approximately 225 million years, and the production of their calcite platelets (coccoliths) contributes to the global carbon cycle over short and geological timescales. Variations in coccolithophore parameters (e.g. community composition, morphology, size and coccolith mass) are a key factor for ocean biogeochemical dynamics (e.g. biological carbon pump) and have been used as a palaeoproxy to understand past oceanographic conditions. Coccolith mass has been frequently estimated with different methods with electron microscopy being the most applied. Here, we compared the electron microscopy (EM) method with the Coulter multisizer (CM) (i.e. electric field disturbance) and bidirectional circular polarization (BCP) methods to estimate coccolith masses (pg CaCO<sub>3</sub>) in controlled laboratory experiments with two ecotypes of *Emiliania huxleyi*. Average coccolith mass estimates were in good agreement with literature data. However, mass estimates from the CM were slightly overestimated compared to EM and BCP estimates, and a correction factor ( $c_f = 0.8$ ) is suggested to compensate for this discrepancy. The relative change in coccolith mass triggered by morphotype-specific structures and environmental parameters (i.e. seawater carbonate chemistry) was suitably captured by each of the three techniques.

### 1 Introduction

The ocean constitutes a crucial part in the biogeochemical cycling of the Earth's elements and represents an important interface between the atmosphere and lithosphere. Phytoplankton are integral to the biogeochemical cycling of the ocean, as they convert inorganic carbon and nutrients into organic compounds through photosynthesis, serving as the foundation for the marine food web and facilitating the transfer of carbon from the atmosphere to the ocean's interior (Litchman et al., 2015). Coccolithophores have been present in Earth's oceans for approximately 225 million years (Not et al., 2012). These organisms produce calcite platelets called coccoliths and sequester significant amounts of calcium carbonate (CaCO<sub>3</sub>) into sea-floor sediments, contributing to the global cycle of carbon and other elements (Neukermans et al., 2023). The geochemical composition of coccoliths can provide valuable insights into the biogeochemical cycles of divalent cations such as magnesium (Mg), strontium (Sr) and barium (Ba) (Müller et al., 2014; Bolton et al., 2016). Changes in morphology, mass and geometry of the intracellularly produced coccoliths has been used to understand palaeoceanographic conditions and investigate the potential influence of this phytoplankton group on climate dynamics and CO<sub>2</sub> fluxes (Renaud and Klaas, 2001; Fielding et al., 2009; Beaufort et al., 2011). Changes in environmental parameters (e.g. salinity, nutrient availability, temperature, carbonate chemistry) can affect the physiology and cell size of coccolithophores and, consequently, has the potential to alter the mass of coccoliths (Fielding et al., 2009; Jin et al., 2016;

Horigome et al., 2014; D’Amario et al., 2018). It has been proposed that coccolith size changes occur proportionally to coccosphere or cell size (Aloisi, 2015; Müller et al., 2021), but this “coccolithophore size rules” hypothesis has been recently challenged and further refined (Suchéras-Marx et al., 2022).

Coccoliths are categorized into holo- and heterococcoliths, depending on life cycle phases and the associated extra- and intracellular biomineralization processes, respectively (Rowson et al., 1986; Young and Henriksen, 2003). Heterococcolith formation occurs in a special cellular compartment within the coccolithophore cell, and completely formed coccoliths are extruded to the cell surface and arranged to compose the coccosphere. The underlying physiological and biogeochemical mechanisms of coccolith formation have been partly revealed (e.g. Mackinder et al., 2011; Mejía et al., 2018), and several hypotheses for the ecological/cellular function of coccolithophore calcification and genesis have been presented (Monteiro et al., 2016; Müller, 2019).

The coccolithophore species *Emiliana huxleyi*, more recently based on genetic arguments also referred to as *Gephyrocapsa huxleyi* (Bendif et al., 2023; Wheeler et al., 2023), is amongst the numerically most abundant and geographically distributed representatives of this functional group in the modern ocean, being an important model species for physiological and biomineralization studies (e.g. Henderiks and Pagani, 2008; Triantaphyllou et al., 2010; Poulton et al., 2011; Müller et al., 2012; Hoffmann et al., 2015; Faucher et al., 2020). In the Southern Ocean, the most dominant ecotypes of *E. huxleyi* are A and BC with distinct differences in their cellular physiology and morphological coccolith structure. The distribution and physiological performance of these ecotypes is determined by temperature, the Antarctic Polar Front and seawater carbonate chemistry (Mohan et al., 2008; Winter et al., 2014; Cubillos et al., 2007; Müller et al., 2015; Charalampopoulou et al., 2016).

The microscopic nature of coccoliths impedes a direct measurement of their mass, and several methods have been applied to indirectly estimate single coccolith masses. Electron microscopy is a powerful technique that uses a beam of electrons to visualize and analyse particles at high resolution. The utilization of electron microscopy has proven to be a valuable technique for measuring the geometry (length, width and thickness) and estimating the mass of coccoliths with the application of geometric constants for specific coccolithophore species and coccolith structures (Young and Ziveri, 2000). The detailed imaging capabilities of electron microscopy reveal the intricate patterns, features and morphology of coccoliths from sediment, ocean and laboratory samples (e.g. Saruwatari et al., 2011). However, electron microscopy requires specialized equipment and experience to differentiate between different coccolith species and to identify any variations in size and morphology, while at the same time sample preparation can be time-consuming and complex.

Another geometric approach to estimate the coccolith mass, especially in laboratory experiments, is the analysis of coccoliths using the Coulter multisizer principle (Müller et al., 2012, 2021). This method is a commonly employed technique in particle measurement, utilizing electrical impedance to ascertain the volume distribution of particles present in a conductive liquid. The Coulter multisizer device is comprised of a small orifice with an applied electric field through which the particle suspension (sample) is passed. As the particles flow through the orifice, they disrupt an electric current that is applied across the orifice. The number, amplitude and duration of disruptions (or pulses) are directly related to the number and volume the analysed particles. The Coulter multisizer principle provides a rapid method to count coccolithophore cells and coccoliths (e.g. Müller et al., 2021), as well as to estimate extracellular CaCO<sub>3</sub> content (Fan et al., 2022) from laboratory samples. Coulter multisizer sample material, however, requires liquid suspension and high particle numbers for appropriate analysis, limiting a generalized application.

The optical properties of coccoliths (i.e. calcite) allow for the application of polarizing or polarized light microscopy for analysis. Utilizing polarized light is an advanced technique that enhances the contrast of images obtained from birefringent materials, demonstrating a heightened level of sensitivity and can be effectively adjusted for both quantitative and qualitative studies. Applications of polarized light microscopy facilitates the recognition and characterization of diverse coccolithophore species (Gordon and Du, 2001; Bollmann, 2014). This method allows for the observation and documentation of the shape, size and arrangement of coccoliths. As a result, it yields valuable taxonomic data and coccolith mass estimations when appropriately calibrated (Beaufort, 2005; Beaufort et al., 2014, 2021; Meier et al., 2014). Certain limitations, however, have been reported for polarized light microscopy and are associated with a particle thickness above 2 µm and with a vertical optical axis orientation of coccolith CaCO<sub>3</sub> crystals (Beaufort et al., 2021).

All three described methods have been applied in coccolithophore studies, but no direct comparison has been reported. Here, coccolith mass estimations derived from electron microscopy, Coulter multisizer and cross-polarized light methodologies are compared using samples from controlled laboratory experiments with two Southern Ocean coccolithophore ecotypes of the species *Emiliana huxleyi*.

## 2 Material and methods

Four Southern Ocean strains of *E. huxleyi* (strains SO 5.14 and SO 5.30 of ecotype A and SO 5.11 and SO 8.15 of ecotype BC, isolated in 2007 by Suellen S. Cook) were grown under nutrient-replete batch-culture conditions at 14 °C in 0.2 µm filtrated natural seawater with a salinity of 35 and a continuous photon flux density of 100 to 115 µmol pho-

tons  $\text{m}^{-2} \text{s}^{-1}$ , assuring desynchronization of the cellular division cycle and independence of sampling time and cellular volume (Müller et al., 2008, 2021). Detailed culture conditions of the experiments (conducted in 2012/2013) are described in Müller et al. (2015). In summary, seawater carbonate chemistry was manipulated for each strain in triplicate treatments to generate a  $p\text{CO}_2$  gradient ranging from 296–1683  $\mu\text{atm}$ , corresponding to a  $\text{pH}_{(\text{total scale})}$  gradient from 8.17 to 7.48. Samples for electron microscopy (EM) and bidirectional circular polarization (BCP) microscopy were pooled for each triplicate treatment and filtered onto polycarbonate filters (0.8  $\mu\text{m}$  pore size) and then dried at 60 °C pending analyses. Samples for coccolith volume were processed directly using a Coulter multisizer 4 (Beckman Coulter Life Sciences) equipped with a 30  $\mu\text{m}$  aperture, calibrated with 5  $\mu\text{m}$  latex particles (NIST traceable standard) and following established protocols (Fan et al., 2022; Faucher et al., 2017; Müller et al., 2012, 2017, 2021).

## 2.1 Scanning electron microscopy

Sample filters were sputter-coated (gold–palladium) and observed on a Hitachi SU-70 field emission scanning electron microscope at the Central Science Laboratory of the University of Tasmania. Images were taken at 1500 $\times$  magnification and analysed using the ImageJ software (Schneider et al., 2012). ImageJ was calibrated using the size bars of the images. Only single coccoliths lying “face up” were analysed for distal shield length (DSL), distal shield width (DSW), central area length (CAL), central area width (CAW), distal shield area (DSA) and the central area area (CAA) (Fig. 1). DSA and the CAA were calculated assuming that both areas are reassembled in a standard elliptical form. Average numbers of 100 and 80 coccoliths were analysed for each geometric parameter of ecotype A and BC, respectively (see the Supplement).

## 2.2 Polarizing microscopy

Sample filters were affixed using a UV optical mounting medium (Norton Optical 74). Employing an automated optical microscope (Leica DM6000) equipped with a 100 $\times$  lens (aperture 1.45), each sample underwent scanning. A blue monochromatic light ( $\lambda = 460 \pm 5 \text{ nm}$ ) was utilized for illumination. Imaging was conducted using a digital camera, SpotFex (Diagnostic Instruments), capturing images of 20 fields of view (FOVs), each measuring 0.0156  $\text{mm}^2$ .

For every FOV, 14 images were acquired, spanning seven focus levels with 700 nm increments. Two polarizing configurations were applied: (1) right circular polarization (RCP) and (2) left circular polarization (LCP), enabling the implementation of the bidirectional circular polarization (BCP) method (Beaufort et al., 2021). The combination of RCP and

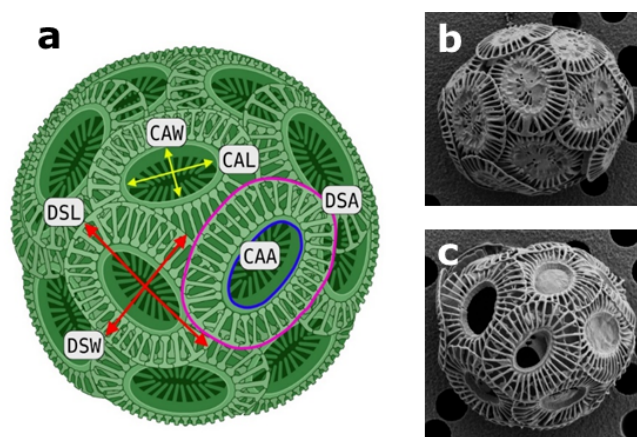


**Figure 1.** Coccospheres of *Emiliana huxleyi*. (a) Schematic illustration of a coccosphere, showcasing the evaluated geometric measurements using scanning electron microscopy (DSL represents distal shield length, DSW represents distal shield width, DSA represents distal shield area, CAL represents central area length, CAW represents central area width, CAA represents central area area). Representative EM images of Southern Ocean *E. huxleyi* ecotype (b) A and (c) BC (Müller et al., 2015).

LCP at each focus level was determined by Eq. (1):

$$d = \frac{\lambda}{\pi \Delta n} \arctan \left( \sqrt{\frac{I_{\text{LR}}}{I_{\text{LL}}}} \right), \quad (1)$$

where  $d$  is the thickness,  $\lambda$  is the wavelength (460 nm),  $\Delta n$  is the birefringence of calcite (0.172), and  $I_{\text{LR}}$  and  $I_{\text{LL}}$  represent grey values measured with right and left circular polarizers, respectively.

After scaling the pixel values of the resulting images by multiplying them by 256 and dividing by 1.34, representing the maximum thickness measured at this wavelength, an 8-bit image was generated, ensuring compatibility with any image analysis program. To enhance focus for each small image segment, the seven images from each FOV were integrated using Helicon Focus software. This calibration process ensured that the light intensity in the resulting FOV image was fully adjusted for 3D imaging, guaranteeing sharp focus across all areas, achieving an accuracy of 0.005  $\mu\text{m}$  for thickness and 0.032  $\text{pg} \mu\text{m}^{-2}$  for mass (Beaufort et al., 2021). Subsequently, the images underwent segmentation and analysis using an AI package called SYRACO (SYstème de Reconnaissance Automatique de COccolithes), which combines morphometry and neural-network-based pattern recognition (Beaufort et al., 2022). SYRACO demonstrated its capability by providing accurate mass and length measurements for *Emiliana huxleyi* coccoliths and coccospheres identified in the scans of the samples.

### 2.3 Coccolith mass estimations

Three methods were used to estimate individual coccolith mass, expressed in pg  $\text{CaCO}_3$ : (1) based on EM, (2) CM and (3) BCP analyses. Coccolith mass from EM analysis was estimated according to the equation:  $\text{mass} = 2.7 \times k_s \times l^3$ , where 2.7 is the density of calcite (in  $\text{g cm}^{-3}$ ),  $k_s$  is a constant dependent on the shape of the coccolith and  $l$  is the distal shield length (Young and Ziveri, 2000). Shape constants were applied after Poulton et al. (2011) with  $k_s = 0.02$  and 0.015 for ecotype A and BC, respectively. Average numbers of 100 and 80 coccoliths were analysed for ecotype A and BC, respectively. Average coccolith volumes obtained with the CM method were extracted from Müller et al. (2017) and transformed into the mass of coccolith by multiplying with the density of calcite. On average, approx.  $6 \times 10^5$  coccoliths were measured per CM sample. Coccolith mass estimates derived from polarizing microscopy (bidirectional circular polarization) analyses followed protocols described in Beaufort et al. (2014, 2021). An average number of 671 coccoliths were analysed per sample to estimate coccolith mass (see the Supplement).

### 2.4 Data and statistical analysis

Possible differences between the two studied strains of each ecotype were analysed by comparing the geometric parameters (derived from electron microscopy analysis) and their linear regressions in regard to seawater  $\text{pH}_t$  between the two individual strains of each ecotype using ANCOVA (analysis of covariance;  $p < 0.05$ ). No significant differences were detected (the Supplement Table S1), and, consequently, the results of the individual strains of each ecotype were pooled and analysed as one data set for each ecotype. Variations of coccolith geometric parameters and mass in regard to seawater pH were analysed by means of linear regression analysis, and significant differences amongst the regression slopes were tested with the “statcalc” software (Soper, 2023). A significance level of 5 % was applied for all statistical analyses.

## 3 Results

All coccolith geometric parameters, derived from electron microscopy (Fig. 1), of both ecotypes were significantly correlated with seawater  $\text{pH}_t$  (Fig. 2 and the Supplement Table S2). Increased coccolith size parameters (DSL, DSW, DSA, CAL, CAW and CAA) were associated with lower seawater  $\text{pH}_t$  values. The data sets of ecotype A and BC were significantly different from each other for all measured geometric parameters (ANCOVA:  $p < 0.05$ ). On the other hand, linear regression slopes of the relations between geometric parameters and  $\text{pH}_t$  were not significantly different between ecotype A and BC with the exception of CAL ( $F = 5.60$ ,  $p = 0.029$ ; Fig. 2e).

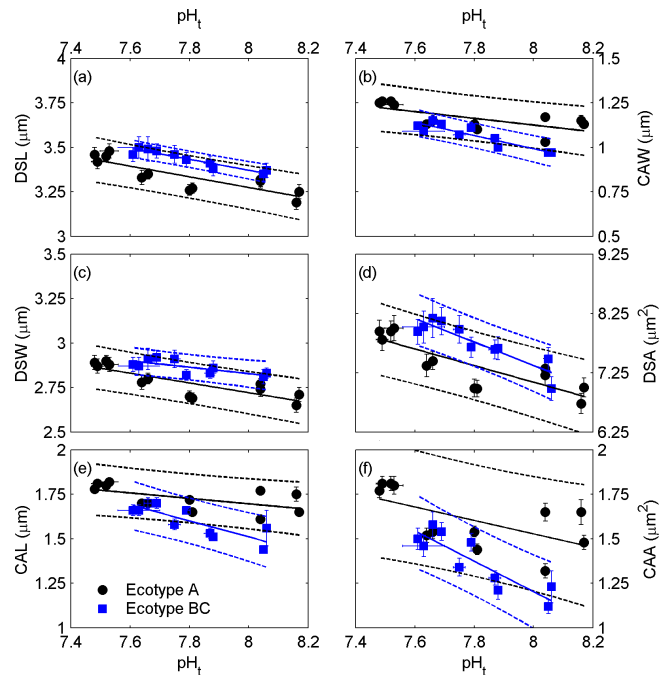


**Figure 2.** Correlations of coccolith size parameters, derived from electron microscopy, to seawater carbonate chemistry, represented by  $\text{pH}_{\text{total scale}} (\pm \text{SD})$ . (a) Distal shield length, (b) central area width, (c) distal shield width, (d) distal shield area, (e) central area length and (f) central area area with corresponding standard errors (SE). Solid lines indicate significant linear regressions ( $p < 0.05$ ) with 95 % prediction intervals (dashed lines).

Ecotype A coccolith mass estimations derived from EM, CM and BCP ranged from 1.83 to 2.37, 2.34 to 2.91, and 1.87 to 2.18 pg  $\text{CaCO}_3$ , respectively, and from 1.59 to 1.85, 2.08 to 2.36, and 1.31 to 2.25 pg  $\text{CaCO}_3$ , respectively, for ecotype BC. Changes in coccolith mass were significantly correlated to seawater  $\text{pH}_{\text{total}}$  with the exception of coccolith mass estimations of ecotype BC derived from CM and BCP measurements (Fig. 3; the Supplement Table S3). For ecotype A, the slopes of the linear regression lines of the CM and BCP methods were not significantly different from the slope of the EM method ( $p > 0.05$ ).

Average coccolith masses over the applied pH gradient were significantly different between the two ecotypes independent of the applied method (Table 1). Average coccolith mass over the applied pH gradient from the CM method was significantly higher than the average values from the other two methods, while no significant differences between the average values of the EM and BCP methods were detected (Table 1).

## 4 Discussion

The results derived from EM indicate a clear influence of seawater carbonate chemistry on coccolith geometry and mass

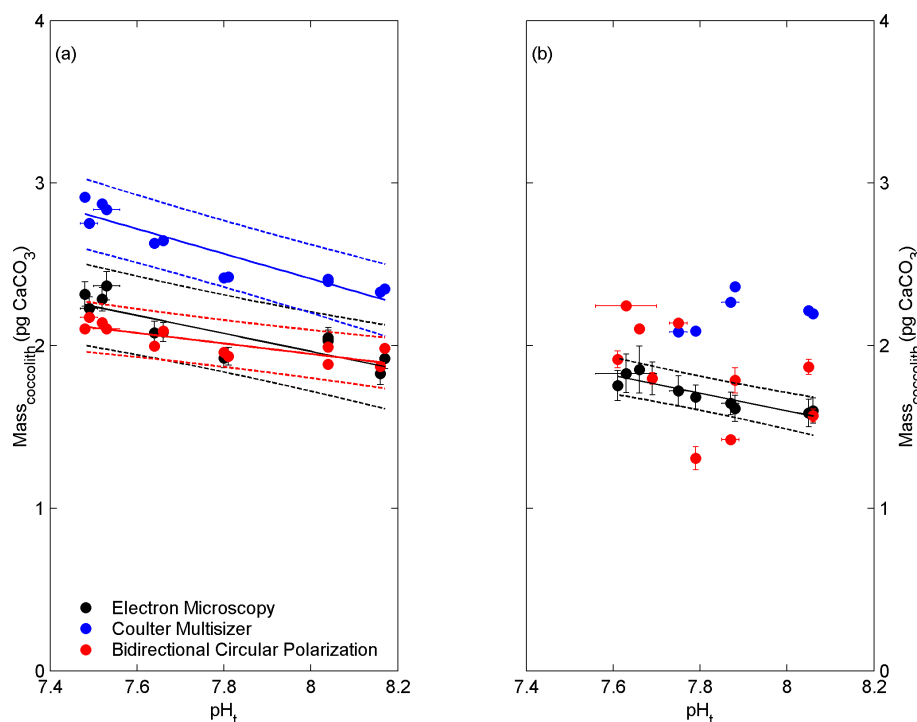


**Figure 3.** Correlations of seawater carbonate chemistry, represented by  $\text{pH}_t$ , to average coccolith mass ( $\pm$  SE) of ecotype A (a) and BC (b). Solid lines indicate significant linear regressions with 95 % prediction intervals (dashed lines).

**Table 1.** Average coccolith mass ( $\pm$  1 SD) of ecotype A and BC over the applied pH gradient. Significant difference between average coccolith mass values of each ecotype and differences amongst the applied method were detected by means of one-way ANOVA.

	Coccolith mass (pg $\text{CaCO}_3$ )		ANOVA <sup>1</sup>
	Ecotype A	Ecotype BC	$p/F$
EM	$2.09 \pm 0.18$ ( $n = 12$ )	$1.71 \pm 0.10$ ( $n = 10$ )	$<0.001/36.7$
CM	$2.58 \pm 0.22$ ( $n = 12$ )	$2.20 \pm 0.11$ ( $n = 6$ )	$0.001/15.6$
BCP	$2.02 \pm 0.10$ ( $n = 12$ )	$1.82 \pm 0.31$ ( $n = 10$ )	$0.042/4.7$
ANOVA <sup>2</sup> $p/F$	$<0.001/37.84^3$	$<0.001/10.96^3$	

EM represents electron microscopy, CM represents Coulter multisizer, BCP represents bidirectional circular polarization. <sup>1</sup> ANOVA testing significant difference between ecotypes. <sup>2</sup> ANOVA testing significant differences amongst applied methods. <sup>3</sup> Mean coccolith mass value from CM analysis was significantly different from EM and BCP analyses, while the difference between EM and BCP was non-significant (post-hoc Tukey honestly significant difference (HSD) test).

estimates (Figs. 2 and 3). The observation of higher coccolith mass in response to lower seawater pH may appear contradictory at first glance as frequently malformed coccoliths are associated with ocean acidification scenarios (e.g. Riebesell et al., 2000). However, this can be rationalized by considering that reduced calcification rates, induced by ocean acidification or reduced seawater pH, are independent of coccolith size (e.g. Müller et al., 2017). The detailed influence of seawater carbonate chemistry on coccolithophore physiology, calcification rates and coccolith geometry has been previously described (Bach et al., 2015; Meyer and Riebesell, 2015; Hermoso and Minoletti, 2018). Instead, this study is focused on the application of three different methods for es-

timating coccolith mass and the implications for future analyses.

The presented data include results from two ecotypes of *E. huxleyi* (i.e. A and BC) from the Southern Ocean. Ecotype BC has been described to produce relatively delicate coccoliths and demonstrates a high physiological sensitivity when exposed to changing environmental conditions compared to the more tolerant ecotype A (Cubillos et al., 2007; Cook et al., 2011, 2013). This is hypothesized to be related to the relatively constant ecological niche of type BC (i.e. the open Southern Ocean) and the evolutionary developed interplay of the underlying genetic and physiological framework (Schluter, 2009; Chevin et al., 2014; Stotz, 2017). The

high sensitivity to low seawater pH of ecotype BC resulted in diminished coccolith production and insufficient sample material for CM analysis at  $\text{pH} < 7.75$  (Fig. 3b).

Three methods (i.e. EM, CM and BCP) were applied to estimate the coccolith mass. All these methods have been previously utilized to estimate coccolith masses from field and laboratory studies, and the individual application procedures are well established and widely reported (see references in Table 2). The average coccolith masses (estimates from the three methods) ranged from 1.59 to 2.91  $\text{pg CaCO}_3$ , which is in good agreement with previously published values from laboratory and field studies, regarding ecotype A and BC (0.9 to 8.2 and 0.6 to 5.1  $\text{pg CaCO}_3$ , respectively; Table 2). Estimates  $> 6 \text{ pg}$  are generally associated with sample material from laboratory experiments, presumably reflecting artificial culture conditions, leading to the formation of unusually large coccoliths (e.g. Müller et al., 2012).

Coccoliths of ecotype BC have a more delicate structure than coccoliths of ecotype A and this is reflected in the lower coccolith mass estimates compared to ecotype A (Fig. 3a and b). This difference was detected to be significant ( $p < 0.05$ ), independent of the applied method (Table 1), indicating comparable method sensitivities for different coccolith shapes of *E. huxleyi*. The non-significant differences between the linear regression slopes of ecotype A (Fig. 3a) further indicates the comparable sensitivity of the three methods to detect changes in coccolith mass induced by seawater carbonate chemistry variations. However, the influence of seawater carbonate chemistry on the coccolith mass of ecotype BC was solely detected with the EM method, which might be related to the coccolith sample size, orientation and morphological quality.

The ecotypes A and BC of *E. huxleyi* produce coccoliths that exhibit gaps lacking calcified structures. The size and number of these gaps are likely an interfering factor for the correct estimation of coccolith mass or  $\text{CaCO}_3$  content. The shape constant ( $k_s$ , applied in the EM method) accounts for the general calcified structure of *E. huxleyi* coccoliths, and it has been estimated to vary between 0.016 and 0.021 for *E. huxleyi* ecotype A (Young and Ziveri, 2000). The shape constants for other *E. huxleyi* ecotypes are given as 0.015 (for ecotype BC; Poulton et al., 2011) and 0.04 for the overcalcified form of ecotype A (Young and Ziveri, 2000), where in the latter the central area (i.e. CAA) is completely calcified. Applying different shape constants to the linear regression models of Fig. 3 generates a comparative overview of the influence of the coccolith shape and degree of calcification on the coccolith mass estimates from electron microscopy (Fig. 4). Interestingly, the coccolith mass estimates (ecotype A) from the CM method are lower than estimates using the shape constant for the overcalcified coccolith structure ( $k_s = 0.04$ ). This indicates that the CM method partly accounts for the structure of the coccoliths of ecotype A and BC, and that possible occlusion (Plaats and Herps, 1984) of the analytical fluid (i.e. seawater) might be responsible for

the observed mass overestimation in comparison to the EM and BCP methods. A correction factor of 0.808 was calculated to fit the estimates derived from EM and BCP by fitting the linear regression of the CM estimates (Fig. 3a) to intersect the linear regression of the EM estimates at  $\text{pH}_t$  of 7.8. Here, a simplified/rounded correction factor ( $c_f$ ) of 0.8 is proposed to be applied to CM coccolith mass estimates (Fig. 4).

Cross-polarized light microscopy can provide information about the crystal orientation and structure of particles (Camaño et al., 2010). It is relatively simple to use and does not require extensive sample preparation but may have limitations in terms of resolution and sensitivity compared to electron microscopy. The resolution of cross-polarized light is constrained by the wavelength of applied light source (typically within the visible range). Consequently, accurately determining the size and shape of particles, particularly smaller ones or those with intricate morphologies (e.g. coccoliths), can be challenging and requires appropriate calibration due to the influence of sample thickness, orientation and particle quality (Çopuroğlu, 2016). The calibration issues of polarizing microscopy have been overcome by the recently developed BCP method (Beaufort et al., 2021) and underlines the valuable application of polarizing microscopy for coccolith analysis, especially in the field of palaeoceanography, where it allows for the examination of crystal orientation and structure of coccoliths extracted from sediments. It is noteworthy that one should be cognizant of each method's limitations and consider employing complementary techniques for a more comprehensive and comparative coccolith analysis to introduce a possible correction factor for the diverse array of coccolithophore morphology and possible refractive properties. Instrumental costs and specific expertise required can differ substantially amongst the applied methods with BCP and EM relying on expensive equipment set-ups and on intense training and expertise compared to the CM method. In laboratory culture studies, however, the CM method offers a fast and cost-effective estimation of coccolith mass from *E. huxleyi*.

In summary, the here-presented results demonstrate that the methods utilized in this study are comparable in terms of their ability to detect alterations in coccolith mass caused by variations in ecotype-specific structure and seawater carbonate chemistry. It should be noted, however, that the Coulter multisizer estimates were slightly overestimated. In order to account for this discrepancy, a unitless correction factor ( $c_f = 0.8$ ) has been proposed. The correction factor is applicable for both tested ecotypes of *E. huxleyi*. This adjustment allows for a high level of comparability between coccolith mass estimates obtained from the three methods and facilitates a future comparison and consolidation of mass changes observed from sediment, oceanographic and laboratory samples.

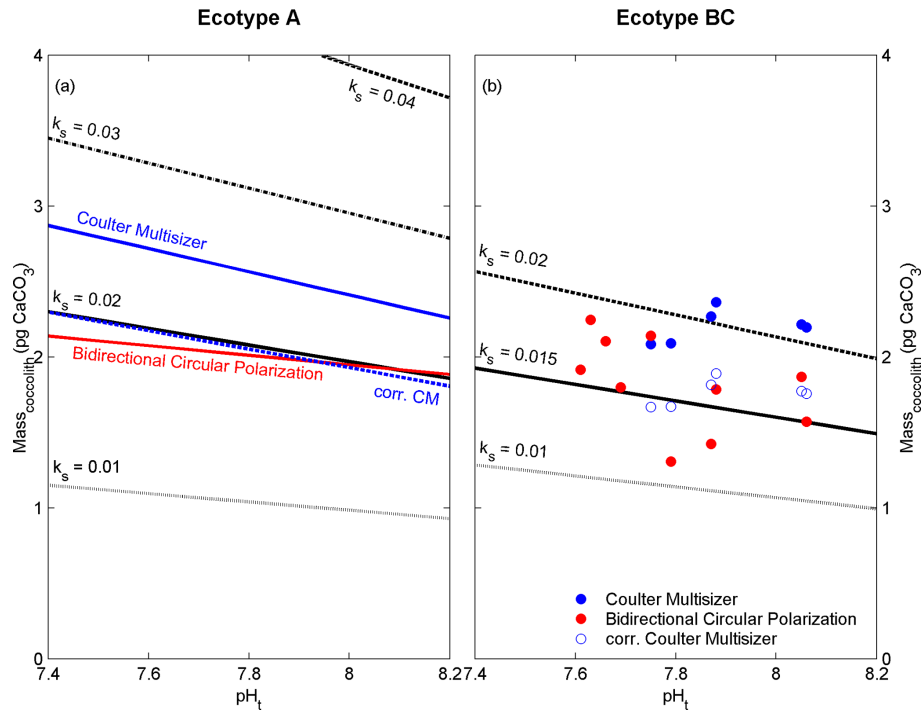


**Figure 4.** Linear regression models or data points of coccolith mass estimates derived from the Coulter multisizer (blue) and cross-polarized light (red) compared to regression models from electron microscopy (black) with different coccolith shape constants ( $k_s$ ) for ecotype A (a) and BC (b). Dashed blue line and open blue dots represent the corrected Coulter multisizer estimates using the  $c_f$  of 0.8 (see text for details).

**Table 2.** Average estimates of *E. huxleyi* coccolith mass from laboratory, seawater and sediment samples. The method category PL (Polarized light) includes different approaches to estimate the coccolith mass using polarizing light microscopy (please refer to each reference for a detailed description). EM represents electron microscopy, CM represents Coulter multisizer, BCP represents bidirectional circular polarization, SYRACO represents SYstème de Reconnaissance Automatique de COccolithes (Beaufort and Dollfus, 2004).

Ecotype and/or origin*	Sample material	Mass (pg CaCO <sub>3</sub> )	Method	Reference
Drake Passage	Sediment	1.6 to 2.4	EM	Vollmar et al. (2022)
Ecotype A/Patagonian Shelf	Seawater	1.2 to 2.6	EM	Poulton et al. (2011)
Ecotype A/Southern Ocean	Laboratory	1.8 to 2.4	EM	This study
Ecotype BC/Patagonian Shelf	Seawater	0.9 to 1.9	EM	Poulton et al. (2011)
Ecotype BC/Southern Ocean	Laboratory	1.6 to 1.9	EM	This study
Ecotype BC/Southern Ocean	Seawater	0.6 to 1.5	EM	Charalampopoulou et al. (2016)
Ecotype A/Norway	Laboratory	1.4 to 7.8	CM	Müller et al. (2012)
Ecotype A/Southern Ocean	Laboratory	2.3 to 2.9	CM	This study
Ecotype BC/Southern Ocean	Laboratory	2.1 to 2.4	CM	This study
Canary Islands	Seawater	1.7 to 2.9	PL	Linge Johnsen and Bollmann (2020)
Subantarctic Zone	Sediment trap	1.8 to 4.3	PL	Rigual-Hernández et al. (2020a)
South of Tasmania	Sediment	2.2 to 3.3	PL	Rigual-Hernández et al. (2020b)
Ecotype A/Southern Ocean	Laboratory	1.9 to 2.2	BCP	This study
Ecotype BC/Southern Ocean	Laboratory	1.3 to 2.2	BCP	This study
South Atlantic and Indian oceans	Sediment	1.7 to 4.9	SYRACO	Horigome et al. (2014)
Mediterranean Sea	Seawater	2.2 to 5.9	SYRACO	D’Amario et al. (2018)
Mediterranean Sea	Sediment trap	2.8 to 5.7	SYRACO	Meier et al. (2014)
Ecotype A/Norway	Laboratory	0.9 to 8.2	SYRACO	Bach et al. (2012)
Ecotype BC/Atlantic Ocean	Laboratory	1.5 to 5.1	SYRACO	Beuvier et al. (2019)

\* Where no ecotype is specified, it is assumed that assemblages of *E. huxleyi* populations were reported containing a mixture of multiple ecotypes.

## 5 Conclusions

Three methods (electron microscopy, Coulter multisizer and bidirectional circular polarization) were applied to estimate the coccolith mass of two laboratory-cultured populations of the coccolithophore *Emiliania huxleyi*. Average coccolith mass estimates are in good agreement with previous studies. However, coccolith mass estimates from the Coulter multisizer were slightly overestimated, and a correction factor has been introduced to compensate for this discrepancy. The relative change in coccolith mass triggered by ecotype-specific structures and seawater carbonate chemistry are suitably captured by each of the three techniques and are comparable. In estimating the absolute values for coccolith mass, it is imperative to exercise prudence when employing the coccolith shape constants and refractory indices, with due consideration for the specific coccolithophore species and their corresponding morphological attributes.

*Code and data availability.* Research data are provided in the paper and the Supplement.

*Supplement.* The supplement related to this article is available online at: <https://doi.org/10.5194/bg-21-1601-2024-supplement>.

*Author contributions.* CRV and MNM designed and conducted the study. LB executed the bidirectional circular polarization analysis. CRV and MNM interpreted the data and wrote the paper with significant comments provided by LB and GMH.

*Competing interests.* The contact author has declared that none of the authors has any competing interests.

*Disclaimer.* Publisher's note: Copernicus Publications remains neutral with regard to jurisdictional claims made in the text, published maps, institutional affiliations, or any other geographical representation in this paper. While Copernicus Publications makes every effort to include appropriate place names, the final responsibility lies with the authors.

*Acknowledgements.* We thank Nick Hayes and James Stone for capturing SEM images at the University of Tasmania. We thank Alex Poulton and one anonymous reviewer for their comments to refine our manuscript.

*Financial support.* This research has been supported by the Australian Research Council (grant no. 1093801) and the Conselho Nacional de Desenvolvimento Científico e Tecnológico (grant no. 305467/2020–4).

*Review statement.* This paper was edited by Emilio Maraón and reviewed by Alex Poulton and one anonymous referee.

## References

- Aloisi, G.: Covariation of metabolic rates and cell size in coccolithophores, *Biogeosciences*, 12, 4665–4692, <https://doi.org/10.5194/bg-12-4665-2015>, 2015.
- Bach, L. T., Bauke, C., Meier, K. J. S., Riebesell, U., and Schulz, K. G.: Influence of changing carbonate chemistry on morphology and weight of coccoliths formed by *Emiliania huxleyi*, *Biogeosciences*, 9, 3449–3463, <https://doi.org/10.5194/bg-9-3449-2012>, 2012.
- Bach, L. T., Riebesell, U., Gutowska, M. A., Federwisch, L., and Schulz, K. G.: A unifying concept of coccolithophore sensitivity to changing carbonate chemistry embedded in an ecological framework, *Prog. Oceanogr.*, 135, 125–138, <https://doi.org/10.1016/j.pocean.2015.04.012>, 2015.
- Beaufort, L.: Weight estimates of coccoliths using the optical properties (birefringence) of calcite, *Micropaleontology*, 51, 289–297, <https://doi.org/10.2113/gsmicropal.51.4.289>, 2005.
- Beaufort, L. and Dollfus, D.: Automatic recognition of coccoliths by dynamical neural networks, *Mar. Micropaleontol.*, 51, 57–73, <https://doi.org/10.1016/j.marmicro.2003.09.003>, 2004.
- Beaufort, L., Probert, I., De Garidel-Thoron, T., Bendif, E. M., Ruiz-Pino, D., Metzl, N., Goyet, C., Buchet, N., Coupel, P., Grelaud, M., Rost, B., Rickaby, R. E. M., and De Vargas, C.: Sensitivity of coccolithophores to carbonate chemistry and ocean acidification, *Nature*, 476, 80–83, <https://doi.org/10.1038/nature10295>, 2011.
- Beaufort, L., Barbarin, N., and Gally, Y.: Optical measurements to determine the thickness of calcite crystals and the mass of thin carbonate particles such as coccoliths, *Nat. Prot.*, 9, 633–642, <https://doi.org/10.1038/nprot.2014.028>, 2014.
- Beaufort, L., Gally, Y., Suchéras-Marx, B., Ferrand, P., and Duboisset, J.: Technical note: A universal method for measuring the thickness of microscopic calcite crystals, based on bidirectional circular polarization, *Biogeosciences*, 18, 775–785, <https://doi.org/10.5194/bg-18-775-2021>, 2021.
- Beaufort, L., Bolton, C. T., Sarr, A. C., Suchéras-Marx, B., Rosenthal, Y., Donnadieu, Y., Barbarin, N., Bova, S., Cornuault, P., Gally, Y., Gray, E., Mazur, J. C., and Tetard, M.: Cyclic evolution of phytoplankton forced by changes in tropical seasonality, *Nature*, 601, 79–84, <https://doi.org/10.1038/s41586-021-04195-7>, 2022.
- Bendif, E. M., Probert, I., Archontikis, O. A., Young, J. R., Beaufort, L., Rickaby, R. E., and Filatov, D.: Rapid diversification underlying the global dominance of a cosmopolitan phytoplankton, *ISME J.*, 17, 630–640, <https://doi.org/10.1038/s41396-023-01365-5>, 2023.
- Beuvier, T., Probert, I., Beaufort, L., Suchéras-Marx, B., Chushkin, Y., Zontone, F., and Gibaud, A.: X-ray nanotomography of coccolithophores reveals that coccolith mass and segment number correlate with grid size, *Nat. Commun.*, 10, 751, <https://doi.org/10.1038/s41467-019-08635-x>, 2019.
- Bollmann, J.: Technical note: weight approximation of coccoliths using a circular polarizer and interference colour derived retar-

- dation estimates – (the cpr method), *Biogeosciences*, 11, 1899–1910, <https://doi.org/10.5194/bg-11-1899-2014>, 2014.
- Bolton, C. T., Hernández-Sánchez, M., Fuertes, M., González-Lemos, S., Abrevaya, L., Mendez-Vicente, A., Flores, J., Probert, I., Giosan, L., Johnson, J., and Stoll, H. M.: Decrease in coccolithophore calcification and CO<sub>2</sub> since the middle miocene, *Nat. Commun.*, 7, 10284, <https://doi.org/10.1038/ncomms10284>, 2016.
- Caamaño, J., Muñoz, M., Díez, C., and Gómez, E.: Polarized light microscopy in mammalian oocytes, *Reprod. Domest. Anim.*, 45, 49–56, <https://doi.org/10.1111/j.1439-0531.2010.01621.x>, 2010.
- Charalampopoulou, A., Poulton, A. J., Bakker, D. C. E., Lucas, M. I., Stinchcombe, M. C., and Tyrrell, T.: Environmental drivers of coccolithophore abundance and calcification across Drake Passage (Southern Ocean), *Biogeosciences*, 13, 5917–5935, <https://doi.org/10.5194/bg-13-5917-2016>, 2016.
- Chevin, L., Decorzent, G., and Lenormand, T.: Niche dimensionality and the genetics of ecological speciation, *Evolution*, 68, 1244–1256, <https://doi.org/10.1111/evo.12346>, 2014.
- Cook, S. S., Whittock, L., Wright, S. W., and Hallegraeff, G. M.: Photosynthetic pigment and genetic differences between two Southern Ocean morphotypes of *Emiliana huxleyi* (Haptophyta), *J. Phycol.*, 47, 615–626, <https://doi.org/10.1111/j.1529-8817.2011.00992.x>, 2011.
- Cook, S. S., Jones, R. C., Vaillancourt, R. E., and Hallegraeff, G. M.: Genetic differentiation among Australian and Southern Ocean populations of the ubiquitous coccolithophore *Emiliana huxleyi* (Haptophyta), *Phycologia*, 52, 368–374, <https://doi.org/10.2216/12-111.1>, 2013.
- Çopuroğlu, O.: Revealing the dark side of portlandite clusters in cement paste by circular polarization microscopy, *Materials*, 9, 176, <https://doi.org/10.3390/ma9030176>, 2016.
- Cubillos, J. C., Wright, S. W., Nash, G., De Salas, M. F., Griffiths, B., Tilbrook, B., Poisson, A., and Hallegraeff, G. M.: Calcification morphotypes of the coccolithophorid *Emiliana huxleyi* in the Southern Ocean: Changes in 2001 to 2006 compared to historical data, *Mar. Ecol. Prog. Ser.*, 348, 47–54, <https://doi.org/10.3354/meps07058>, 2007.
- D'Amario, B., Ziveri, P., Grelaud, M., and Oviedo, A.: *Emiliana huxleyi* coccolith calcite mass modulation by morphological changes and ecology in the Mediterranean Sea, *Plos One*, 13, e0201161, <https://doi.org/10.1371/journal.pone.0201161>, 2018.
- Fan, X., Batchelor-McAuley, C., Yang, M., Barton, S. G., Rickaby, R. E. M., Bouman, H. A., and Compton, R. G.: Quantifying the extent of calcification of a coccolithophore using a coulter counter, *Anal. Chem.*, 94, 12664–12672, <https://doi.org/10.1021/acs.analchem.2c01971>, 2022.
- Faucher, G., Hoffmann, L., Bach, L. T., Bottini, C., Erba, E., and Riebesell, U.: Impact of trace metal concentrations on coccolithophore growth and morphology: laboratory simulations of Cretaceous stress, *Biogeosciences*, 14, 3603–3613, <https://doi.org/10.5194/bg-14-3603-2017>, 2017.
- Faucher, G., Riebesell, U., and Bach, L. T.: Can morphological features of coccolithophores serve as a reliable proxy to reconstruct environmental conditions of the past?, *Clim. Past*, 16, 1007–1025, <https://doi.org/10.5194/cp-16-1007-2020>, 2020.
- Fielding, S. R., Herrle, J. O., Bollmann, J., Worden, R. H., and Montagnés, D. J. S.: Assessing the applicability of *Emiliana huxleyi* coccolith morphology as a sea-surface salinity proxy, *Limnol. Oceanogr.*, 54, 1475–1480, <https://doi.org/10.4319/lo.2009.54.5.1475>, 2009.
- Gordon, H. and Du, T.: Light scattering by nonspherical particles: application to coccoliths detached from *Emiliana huxleyi*, *Limnol. Oceanogr.*, 46, 1438–1454, <https://doi.org/10.4319/lo.2001.46.6.1438>, 2001.
- Henderiks, J. and Pagani, M.: Coccolithophore cell size and the Paleogene decline in atmospheric CO<sub>2</sub>, *Earth Planet. Sc. Lett.*, 269, 576–584, <https://doi.org/10.1016/j.epsl.2008.03.016>, 2008.
- Hermoso, M. and Minoletti, F.: Mass and fine-scale morphological changes induced by changing seawater pH in the coccolith *Gephyrocapsa oceanica*, *J. Geophys. Res.-Biogeo.*, 123, 2761–2774, <https://doi.org/10.1029/2018jg004535>, 2018.
- Hoffmann, R., Kirchlechner, C., Langer, G., Wochnik, A. S., Griesshaber, E., Schmahl, W. W., and Scheu, C.: Insight into *Emiliana huxleyi* coccospheres by focused ion beam sectioning, *Biogeosciences*, 12, 825–834, <https://doi.org/10.5194/bg-12-825-2015>, 2015.
- Horigome, M. T., Ziveri, P., Grelaud, M., Baumann, K.-H., Marino, G., and Mortyn, P. G.: Environmental controls on the *Emiliana huxleyi* calcite mass, *Biogeosciences*, 11, 2295–2308, <https://doi.org/10.5194/bg-11-2295-2014>, 2014.
- Jin, X., Liu, C., Poulton, A., Dai, M., and Guo, X.: Coccolithophore responses to environmental variability in the south china sea: species composition and calcite content, *Biogeosciences*, 13, 4843–4861, <https://doi.org/10.5194/bg-13-4843-2016>, 2016.
- Linge Johnsen, S. A. and Bollmann, J.: Coccolith mass and morphology of different *Emiliana huxleyi* morphotypes: A critical examination using Canary Islands material, *Plos One*, 15, e0230569, <https://doi.org/10.1371/journal.pone.0230569>, 2020.
- Litchman, E., Pinto, P. d. T., Edwards, K. F., Klausmeier, C. A., Kremer, C. T., and Thomas, M. K.: Global biogeochemical impacts of phytoplankton: a trait-based perspective, *J. Ecol.*, 103, 1384–1396, <https://doi.org/10.1111/1365-2745.12438>, 2015.
- Mackinder, L., Wheeler, G., Schroeder, D., von Dassow, P., Riebesell, U., and Brownlee, C.: Expression of biomineralization-related ion transport genes in *Emiliana huxleyi*, *Environ. Microbiol.*, 13, 3250–3265, <https://doi.org/10.1111/j.1462-2920.2011.02561.x>, 2011.
- Meier, K. J. S., Beaufort, L., Heussner, S., and Ziveri, P.: The role of ocean acidification in *Emiliana huxleyi* coccolith thinning in the Mediterranean Sea, *Biogeosciences*, 11, 2857–2869, <https://doi.org/10.5194/bg-11-2857-2014>, 2014.
- Mejía, L. M., Paytan, A., Eisenhauer, A., Böhm, F., Kolevica, A., Bolton, C., Méndez-Vicente, A., Abrevaya, L., Isensee, K., and Stoll, H.: Controls over  $\delta^{44}/^{40}\text{Ca}$  and Sr/Ca variations in coccoliths: New perspectives from laboratory cultures and cellular models, *Earth Planet. Sc. Lett.* 481, 48–60, <https://doi.org/10.1016/j.epsl.2017.10.013>, 2018.
- Meyer, J. L. and Riebesell, U.: Reviews and syntheses: responses of coccolithophores to ocean acidification: a meta-analysis, *Biogeosciences*, 12, 1671–1682, <https://doi.org/10.5194/bg-12-1671-2015>, 2015.
- Mohan, R., Mergulhao, L. P., Guptha, M. V. S., Rajakumar, A., Thamban, M., AnilKumar, N., Sudhakar, M., and Ravindra, R.: Ecology of coccolithophores in the Indian sector of the Southern Ocean, *Mar. Micropaleontol.*, 67, 30–45, <https://doi.org/10.1016/j.marmicro.2007.08.005>, 2008.

- Monteiro, F. M., Bach, L. T., Brownlee, C., Bown, P., Rickaby, R. E., Poulton, A. J., Tyrrell, T., Beaufort, L., Dutkiewicz, S., Gibbs, S., Gutowska, M. A., Lee, R., Riebesell, U., Young, J., and Ridgwell, A.: Why marine phytoplankton calcify, *Sci. Adv.*, 2, e1501822, <https://doi.org/10.1126/sciadv.1501822>, 2016.
- Müller, M. N., Antia, A. N., and LaRoche, J.: Influence of cell cycle phase on calcification in the coccolithophore *Emiliana huxleyi*, *Limnol. Oceanogr.*, 53, 506–512, <https://doi.org/10.4319/lo.2008.53.2.0506>, 2008.
- Müller, M. N., Beaufort, L., Bernard, O., Pedrotti, M. L., Talec, A., and Sciandra, A.: Influence of CO<sub>2</sub> and nitrogen limitation on the coccolith volume of *Emiliana huxleyi* (Haptophyta), *Biogeosciences*, 9, 4155–4167, <https://doi.org/10.5194/bg-9-4155-2012>, 2012.
- Müller, M. N., Lebrato, M., Riebesell, U., Barcelos e Ramos, J., Schulz, K. G., Blanco-Ameijeiras, S., Sett, S., Eisenhauer, A., and Stoll, H. M.: Influence of temperature and CO<sub>2</sub> on the strontium and magnesium composition of coccolithophore calcite, *Biogeosciences*, 11, 1065–1075, <https://doi.org/10.5194/bg-11-1065-2014>, 2014.
- Müller, M. N., Trull, T. W., and Hallegraef, G. M.: Differing responses of three Southern Ocean *Emiliana huxleyi* ecotypes to changing seawater carbonate chemistry, *Mar. Ecol. Prog. Ser.*, 531, 81–90, <https://doi.org/10.3354/meps11309>, 2015.
- Müller, M. N., Trull, T. W., and Hallegraef, G. M.: Independence of nutrient limitation and carbon dioxide impacts on the Southern Ocean coccolithophore *Emiliana huxleyi*, *ISME J.*, 11, 1777–1787, <https://doi.org/10.1038/ismej.2017.53>, 2017.
- Müller, M. N.: On the Genesis and Function of Coccolithophore Calcification, *Front. Mar. Sci.*, 6, 1–5, <https://doi.org/10.3389/fmars.2019.00049>, 2019.
- Müller, M. N., Brandini, F. P., Trull, T. W., and Hallegraef, G. M.: Coccolith volume of the Southern Ocean coccolithophore *Emiliana huxleyi* as a possible indicator for palaeo-cell volume, *Geobiology*, 19, 63–74, <https://doi.org/10.1111/gbi.12414>, 2021.
- Neukermans, G., Bach, L. T., Butterley, A., Sun, Q., Claustre, H., and Fournier, G.: Quantitative and mechanistic understanding of the open ocean carbonate pump – perspectives for remote sensing and autonomous in situ observation, *Earth-Sci. Rev.*, 239, 104359, <https://doi.org/10.1016/j.earscirev.2023.104359>, 2023.
- Not, F., Gachon, C. M. M., Kooistra, W. H. C. F., Simon, N., Vaulot, D., and Probert, I.: Diversity and ecology of eukaryotic marine phytoplankton, *Adv. Bot. Res.*, 64, 1–53, <https://doi.org/10.1016/b978-0-12-391499-6.00001-3>, 2012.
- Plaats, G. v. d. and Herps, H.: A study on the sizing process of an instrument based on the electrical sensing zone principle, Part 2. The influence of particle porosity, *Powder Technol.*, 38, 73–76, [https://doi.org/10.1016/0032-5910\(84\)80035-2](https://doi.org/10.1016/0032-5910(84)80035-2), 1984.
- Poulton, A. J., Young, J. R., Bates, N. R., and Balch, W. M.: Biometry of detached *Emiliana huxleyi* coccoliths along the Patagonian Shelf, *Mar. Ecol. Prog. Ser.*, 443, 1–17, <https://doi.org/10.3354/meps09445>, 2011.
- Renaud, S. and Klaas, C.: Seasonal variations in the morphology of the coccolithophore *Calcidiscus leptoporus* off Bermuda (N. Atlantic), *J. Plankton Res.*, 23, 779–795, <https://doi.org/10.1093/plankt/23.8.779>, 2001.
- Riebesell, U., Zondervan, I., Rost, B., Tortell, P. D., Zeebe, R. E., and Morel, F. M. M.: Reduced calcification of marine plankton in response to increased atmospheric CO<sub>2</sub>, *Nature*, 407, 364–367, <https://doi.org/10.1038/35030078>, 2000.
- Rigual-Hernández, A. S., Sánchez-Santos, J. M., Eriksen, R., Moy, A. D., Sierro, F. J., Flores, J. A., Abrantes, F., Bostock, H., Nodder, S. D., González-Lanchas, A., and Trull, T. W.: Limited variability in the phytoplankton *Emiliana huxleyi* since the pre-industrial era in the Subantarctic Southern Ocean, *Anthropocene*, 31, 100254, <https://doi.org/10.1016/j.ancene.2020.100254>, 2020a.
- Rigual-Hernández, A. S., Trull, T. W., Flores, J. A., Nodder, S. D., Eriksen, R., Davies, D. M., Hallegraef, G. M., Sierro, F. J., Patil, S. M., Cortina, A., Ballegeer, A. M., Northcote, L. C., Abrantes, F., and Rufino, M. M.: Full annual monitoring of Subantarctic *Emiliana huxleyi* populations reveals highly calcified morphotypes in high-CO<sub>2</sub> winter conditions, *Sci. Rep.*, 10, 2594, <https://doi.org/10.1038/s41598-020-59375-8>, 2020b.
- Rowson, J. D., Leadbeater, B. S. C., and Green, J. C.: Calcium carbonate deposition in the motile (*Crystallolithus*) phase of *Coccolithus pelagicus* (Prymnesiophyceae), *Br. Phycol. J.*, 21, 359–370, <https://doi.org/10.1080/00071618600650431>, 1986.
- Saruwatari, K., Nagasaka, S., Ozaki, N., and Nagasawa, H.: Morphological and crystallographic transformation from immature to mature coccoliths, *Pleurochrysis carterae*, *Mar. Biotechnol.*, 13, 801–809, <https://doi.org/10.1007/s10126-010-9342-7>, 2011.
- Schneider, C. A., Rasband, W. S., and Eliceiri, K. W.: NIH Image to ImageJ: 25 years of image analysis, *Nat. Methods*, 9, 671–675, <https://doi.org/10.1038/nmeth.2089>, 2012.
- Schluter, D.: Evidence for ecological speciation and its alternative, *Science*, 323, 737–741, <https://doi.org/10.1126/science.1160006>, 2009.
- Soper, D. S.: Significance of the Difference between Two Slopes Calculator [software], <https://www.danielsoper.com/statcalc>, last access: 9 December 2023.
- Stotz, K.: Why developmental niche construction is not selective niche construction: and why it matters, *Interface Focus*, 7, 20160157, <https://doi.org/10.1098/rsfs.2016.0157>, 2017.
- Suchéras-Marx, B., Viseur, S., Walker, C. E., Beaufort, L., Probert, I., and Bolton, C. T.: Coccolith size rules – what controls the size of coccoliths during coccolithogenesis?, *Mar. Micropaleontol.*, 170, 102080, <https://doi.org/10.1016/j.marmicro.2021.102080>, 2022.
- Triantaphyllou, M., Dimiza, M., Krasakopoulou, E., Malinverno, E., Lianou, V., and Souvermezoglou, E.: Seasonal variation in *Emiliana huxleyi* coccolith morphology and calcification in the Aegean Sea (Eastern Mediterranean), *Geobios*, 43, 99–110, <https://doi.org/10.1016/j.geobios.2009.09.002>, 2010.
- Vollmar, N., Baumann, K., Saavedra-Pellitero, M., and Hernández-Almeida, I.: Distribution of coccoliths in surface sediments across the Drake passage and calcification of *Emiliana huxleyi* morphotypes, *Biogeosciences*, 19, 585–612, <https://doi.org/10.5194/bg-19-585-2022>, 2022.
- Wheeler, G. L., Sturm, D., and Langer, G.: *Gephyrocapsa huxleyi* (*Emiliana huxleyi*) as a model system for coccolithophore biology, *J. Phycol.*, 59, 1123–1129, <https://doi.org/10.1111/jpy.13404>, 2023.
- Winter, A., Henderiks, J., Beaufort, L., Rickaby, R. E. M., and Brown, C. W.: Poleward expansion of the coccolithophore *Emiliana huxleyi*, *J. Plankton Res.*, 36, 316–325, <https://doi.org/10.1093/plankt/fbt110>, 2014.

Young, J. R. and Henriksen, K.: Biomineralization Within Vesicles: The Calcite of Coccoliths, *Rev. Mineral. Geochem.*, 54, 189–215, <https://doi.org/10.2113/0540189>, 2003.

Young, J. R. and Ziveri, P.: Calculation of coccolith volume and its use in calibration of carbonate flux estimates, *Deep-Sea Res. Pt. II*, 47, 1679–1700, [https://doi.org/10.1016/S0967-0645\(00\)00003-5](https://doi.org/10.1016/S0967-0645(00)00003-5), 2000.